Research on a Superconducting Synchronous Generator for Wind Power

Cheng Wen and Xiaoyun Sun[*]

Abstract—A superconducting synchronous generator (SSG) is proposed for wind power, in which magnesium diboride (MgB_2) superconducting coils are employed as field windings. The stator is composed of conventional copper coils and iron core, while the rotor has no iron core. The whole refrigeration method is adopted in this paper. The thermal barrier is not placed in between the stator and the rotor as compared with the prior HTS generators, so a small air gap width would be possible. In order to study the electromagnetic characteristics of the SSG, finite element method (FEM) is implemented to optimize the SSG and obtain the no-load and load performance of the initial and optimized SSG. Finally, the optimized SSG is compared with a traditional synchronous generator (TSG) of the same power. The results indicate that the optimized SSG has many merits such as small size, light weight, high efficiency and high power factor.

1. INTRODUCTION

A traditional megawatt wind turbine generator is not only heavy but also bulky, which brings inconveniences in installation and maintenance [1]. Since the discovery of high temperature superconductor (HTS) in 1986, the development of HTS material has been rapid. Many breakthroughs for HTS generator have been achieved. HTS synchronous generator is smaller and lighter than the conventional generator of the same power due to high current carrying capacity and negligible DC losses of HTS [2]. At present, the YBCO or Bi-2223 HTS material is employed as the field winding in most HTS synchronous generators [3–5]. However, their high cost has prevented them from being applied to the cost-sensitive wind energy market.

The magnesium diboride (MgB_2), which was discovered at the early twenty-first century, is a metallic superconductor. Its transition temperature is up to 39 K [6]. Compared with any oxide HTS material, MgB_2 wires have the advantage of high critical current density, low cost and simple manufacturing process. Moreover, it can be bent freely like copper wire because of very small bending radius. The main weakness of MgB_2 wires is the relatively low critical temperature. However, with the continued development of refrigeration technology, MgB_2 will become a very promising superconductor.

The refrigeration technology is the key to allow HTS generator to run normally. For most current methods, the insulation blanket is placed in between the stator and rotor for generators with HTS field windings [7, 8]. The insulation blanket must occupy a certain space, so the air gap distance will increase. This structure will seriously influence the performance and efficiency of HTS generator. Therefore, a reasonable cooling system has been one of the focuses and difficult problems in the research of HTS electrical machine.

In this paper, MgB_2 superconducting wires are employed as the field windings of a superconducting synchronous generator (SSG). The whole refrigeration method is adopted. The whole refrigeration method is that the insulation blanket is placed with the outermost layer of HTS generator. The stator

[*] Corresponding author: Xiaoyun Sun (sunxyheb@astdu.edu.cn).
The authors are with the Institute of Electrical and Electronic Engineering, ShiJiangzhuang Tiedao University, China.

and rotor are wrapped in it. The thermal barrier is not placed in between the stator and rotor, but a layer of thin film is pasted on the tooth surface of the stator to prevent thermal radiation. Not only does this method not affect the performance and efficiency of HTS generator, but also it makes the structure of HTS generator more compact and the copper loss decrease greatly. The finite element method (FEM) is implemented to optimize the SSG and obtain the no-load and load performance of the initial and optimized SSG. Finally, the SSG is compared with a traditional synchronous generator (TSG) of the same power.

2. BASIC STRUCTURE OF SSG

In this paper the structure of SSG is similar to that of conventional synchronous machine, so that we can use it for referencing the design method of a conventional machine. This structure is a main choice of superconducting generators developed in the world.

2.1. Structure of Stator

The stator of SSG has two kinds of structure, namely, slotted and unslotted ones. Armature winding is installed between the rotor and ferromagnetic shielding when the stator has unslotted structure. It looks like working in the air gap of a conventional generator. So it can be called air-gap winding. That structure has merits of good air gap flux density waveform, small harmonic loss, low noise, etc. It can better reflect the advantage of a superconducting generator. However, the structure has no core tooth, and other measures must be taken to fix the straight line part of the armature windings. The armature windings in the main magnetic field directly bear the total electromagnetic torque of the generator. Moreover, this structure has less application in the conventional generator. Mechanical stress, cooling methods, technology and other issues are needed for further research due to no mature experience for reference.

Considering the aim of this study, the manufacturing difficulty and cost, the stator core of SSG employs a traditional cogging structure. This structure has certain advantages, but it brings a serious problem, which is that the waveform of air gap flux density can produce a large number of harmonics due to traditional cogging structure, so this problem can be considered as the focus of subsequent optimization.

2.2. Structure of Rotor

The rotor of SSG has two kinds of structure, namely, cored and ironless ones. The cored magnet introduces part of core in the superconducting magnet. This scheme has the advantage of good air gap flux density waveform and magnetic field distribution, and its disadvantage is that the iron core is likely to saturate with the increase of air gap flux density. In addition, compared with a traditional generator, the large capacity of the superconducting generator is not so powerful. Therefore, the rotor of SSG uses an ironless structure in order to better reflect the advantages of superconductor in this paper. The bracket of superconducting magnet uses a material with poor permeability and good heat conductivity, for example, titanium alloy or aluminum alloy.

Superconducting magnets are composed of MgB_2 wires with the same specifications in the form of a racetrack. The bending radius will always be present in each superconducting material, but the size of bending radius is different. The superconducting coils are winded on the skeleton similar to racetrack, as shown in Fig. 1(a). Compared with any oxide HTS material, MgB_2 coils can be bent freely like copper wire because of very small bending radius. A more suitable way is designed based on the racetrack coil in this paper, which is that the superconducting field coils are winded on the pole shoe. The lower end of the pole shoe is similar to the rectangular columns, both ends of which are in a circular arc shape. So it will not have a too small bending radius, as shown in Fig. 1(b). The pole shoe is turned 180 degrees when the superconducting field coils are winded.

The rotating shaft of SSG employs a hollow shaft. Cold air is pumped into to the hollow shaft for cooling superconducting magnets. The rotating shaft uses a material with resistance to low temperature and poor heat conductivity because the rotating shaft is connected with the outside world, for example, glass reinforced plastic.
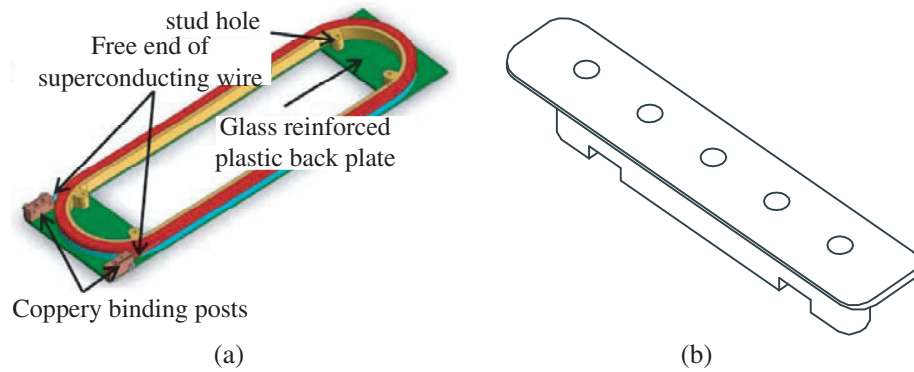
Figure 1. (a) Racetrack coil. (b) Pole shoe of SSG.

2.3. Cooling System

The whole cooling method is adopted in this paper. The thermal barrier is not placed between the stator and rotor, but a layer of thin film is pasted on the tooth surface of the stator to prevent thermal radiation. Not only does this method not affect the performance and efficiency of SSG, but also the structure of SSG is made more compact; besides, the copper loss decreases greatly for SSG with the conventional stator. The common cooling method for the SSG is that the rotor with the superconducting field winding is sealed and run in low temperature, while the stator is run at room temperature. A problem with the common cooling method is that the dynamic seal cannot work continuously for several thousands of hours. However, the whole cooling method can avoid the problem. The whole cooling method is theoretically feasible in long continuous operation. The design is described as below.

A copper tube is placed at the bottom of each slot in stator, and each side of the copper tube is connected with an isolation sleeve. The isolation sleeve is designed to prevent the formation of eddy current loss in the copper tube. Finally, the isolation sleeves are connected with the bus tube, as shown in Fig. 2(a). In addition, a layer of toroidal solenoid is rounded on the shell of SSG, as shown in Fig. 2(b).

To restrain costs, the stator is cooled by liquid nitrogen flowing into a copper tube in each slot of the stator and the toroidal solenoid on the shell of SSG. The temperature of stator area can be kept between 70 and 100 K. Therefore, the copper loss is greatly decreased. Moreover, the rotor is cooled by helium gas flowing into the spindle. Its operating temperature is 20 K, while the temperature of stator area is significantly higher than the operating temperature of the rotor. Therefore, a layer of teflon thin film is pasted on the tooth surface of the stator for preventing thermal radiation.

In general, the structure of SSG mainly includes three parts: stator, rotor and cooling system. The explosive-assembly of SSG is shown in Fig. 3.
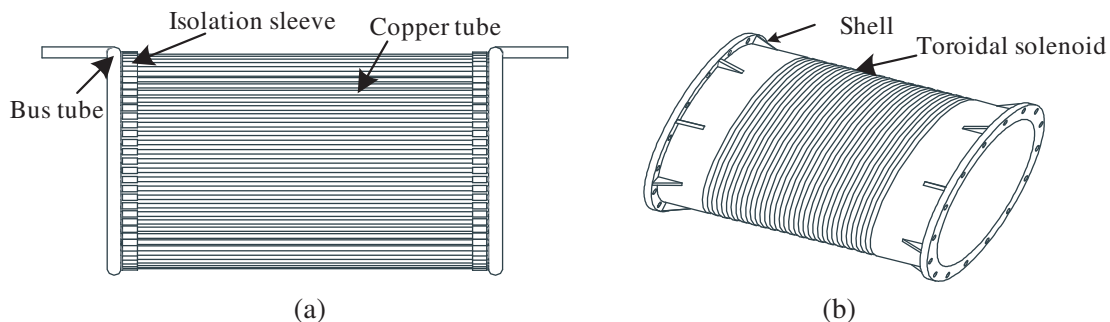
Figure 2. (a) Basic structure of cooling pipe. (b) Structure schematic of the shell.
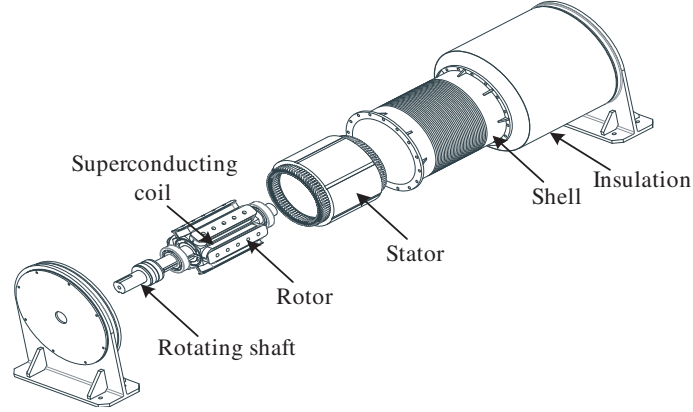
Figure 3. Explosive-assembly of SSG.

3. ELECTROMAGNETIC ANALYSIS

The two-dimensional image and simplified cross-sectional view of SSG is shown in Fig. 4(a). R_1 and R_2 are inside and outside radii of rotor, respectively, while R_3 and R_4 are inside and outside radii of stator, respectively. The entire space of SSC is divided into three areas, namely: I, II, III, which are in correspondence with the air gap, rotor and stator, as shown in Fig. 4(b).

(a)   (b)
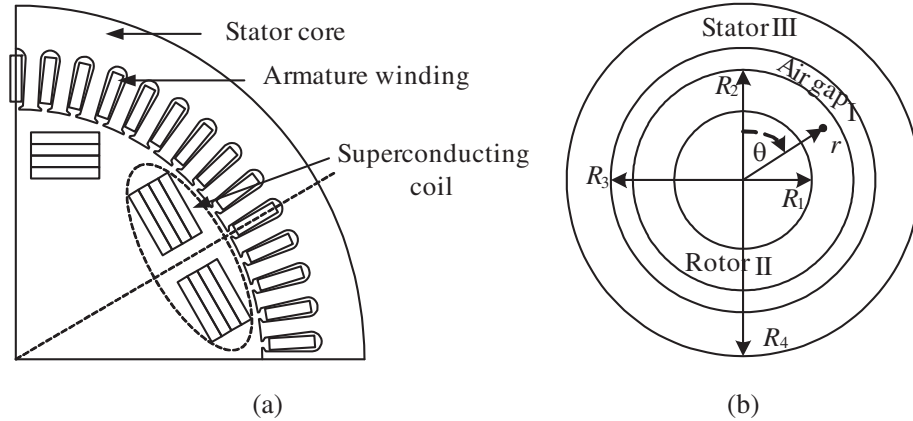
Figure 4. (a) Two-dimensional image. (b) Simplified cross-sectional view.

The following formula can be given according to the Maxwell equations.

$$-\nabla^2 \vec{A} = \mu \vec{J} \tag{1}$$

where $\vec{A}$ is the magnetic vector potential, $\vec{J}$ the current density, and μ the magnetic permeability. The detailed deducing of Equation (1) is given in [9].

When the SSG is in idle run, the following formula can be derived according to Equation (1).

$$\begin{cases} \nabla^2 A_I = 0 & R_2 \leq r \leq R_3 \\ \nabla^2 A_{II} = -\mu_0 J_s & R_1 \leq r \leq R_2 \\ \nabla^2 A_{III} = 0 & R_3 \leq r \leq R_4 \end{cases} \tag{2}$$

where μ_0 is the permeability of vacuum, and J_s is the current density of SM. Equation (2) shows that the two-dimensional electromagnetic problem of the SSG can be boiled down to the mathematical problems

of solving Laplace equation in areas I and III, as well as solving poisson equation in area II. In polar coordinates, Equation (2) can be written as follows.

$$\begin{cases} \dfrac{\partial^2 A_I}{\partial r^2} + \dfrac{1}{r}\dfrac{\partial A_I}{\partial r} + \dfrac{1}{r^2}\dfrac{\partial^2 A_I}{\partial \theta^2} = 0 & R_2 \le r \le R_3 \\[2mm] \dfrac{\partial^2 A_{II}}{\partial r^2} + \dfrac{1}{r}\dfrac{\partial A_{II}}{\partial r} + \dfrac{1}{r^2}\dfrac{\partial^2 A_{II}}{\partial \theta^2} = -\mu_0 J_s & R_1 \le r \le R_2 \\[2mm] \dfrac{\partial^2 A_{III}}{\partial r^2} + \dfrac{1}{r}\dfrac{\partial A_{III}}{\partial r} + \dfrac{1}{r^2}\dfrac{\partial^2 A_{III}}{\partial \theta^2} = 0 & R_3 \le r \le R_4 \end{cases} \quad (3)$$

Then, the finite element (FE) calculation is performed according to the boundary conditions.

4. ELECTROMAGNETIC DESIGN OF SSG

In the paper, a 1.5 MW SSG is used as the research model. An existing stator is employed for cost savings. The existing stator is taken from a conventional motor made in the previous project. The basic design parameters are summarized in Table 1.

Table 1. Specification of the SSG.

Type	3-phase synchronous generator
Rated power	1.5 MW
Rated revolution	20 rpm
Rated voltage	3.8 kV
Rated current	227.3 A
Current density of field coils	0.8×10^8 A/m^2
Operating temperature	20 K
Slot number	108
Inner radius of stator iron	650 mm
Outer radius of stator iron	890 mm

Based on the design principles mentioned before, the initial structure of SSG is obtained, as shown in Fig. 5. MgB$_2$ superconducting wires are employed to wind the SM in this paper. The outer diameter and cross-sectional area of insulated MgB$_2$ superconducting wires are 1.6 mm and 2 mm^2, respectively. $d1$, $d2$, $d3$ and $d4$ are half of the inter width of field coils, respectively.

4.1. Air-Gap Flux Density Distribution

The cross-sectional shape of the field winding could also affect the air gap magnetic flux density (AGMFD) of the HTS generator with a coreless rotor and an existing stator. The AGMFD waveform can seriously influence the performance of generator, especially the voltage waveform which is of primary concern for a successful generator. In the SSG, as mentioned above, the stator is taken from the existing motor. So the improvement of the stator is impossible. However, the rotor has no core. Thus, the total harmonic distortion (THD) of the AGMFD can only be reduced by optimizing the cross-sectional shape of the MgB$_2$ field coils.

Figure 6(a) shows the AGMFD distribution for the initial cross-section shape of field coils. It is clear that the AGMFD waveform is a non-sinusoidal wave. Fig. 6(b) shows the fast Fourier transform (FFT) result of the AGMFD waveform. Compared with fundamental component, the 3rd and 5th order harmonics are large. The THD is 32.48%.

$d2$, $d3$, and $d4$ remain unchanged, thus the AGMFD waveform changes with $d1$. Then the relation curve of THD and $d1$ can be obtained by harmonic analysis for the waveform. Same as the above principle, the relation curves of THD and $d2$, $d3$, and $d4$ can be obtained and shown as in Fig. 7.
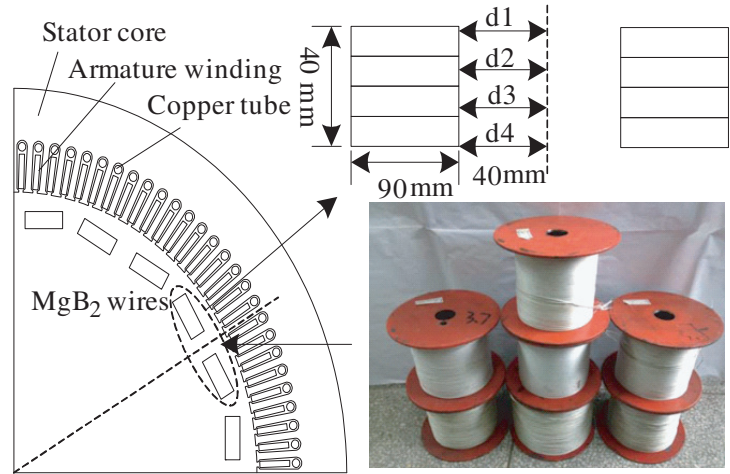
Figure 5. Initial cross-sectional illustration of SSG.

(a)   (b)
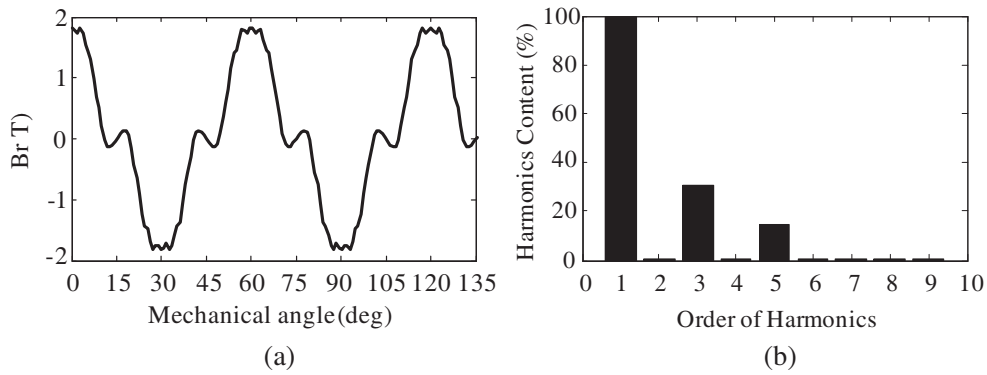
Figure 6. (a) AGMFD distribution for initial shape of field coils. (b) Corresponding FFT result.
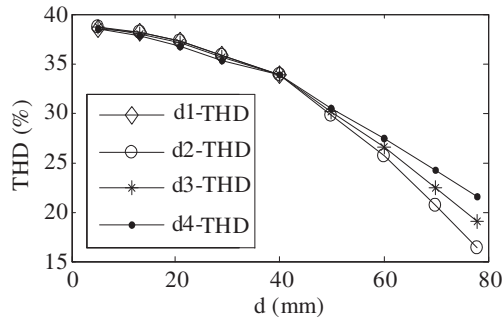
Figure 7. Dependencies of THD on $d1$, $d2$, $d3$, $d4$ for AGMFD.

The above result is obtained by changing one variable. When the four variables are changed together, a great deal of FE calculation will be required to find the minimum THD.

4.2. Optimal Design

The FEM is implemented to optimize the SSG in this paper. The objective function of optimization is to minimize the THD of the AGMFD waveform. The design variables are $d1$, $d2$, $d3$, and $d4$ respectively. The constraints of design variables are listed below: $5\,\text{mm} < d1 < 45\,\text{mm}$, $5\,\text{mm} < d2 < 80\,\text{mm}$, $5\,\text{mm} < d3 < 80\,\text{mm}$, $5\,\text{mm} < d4 < 78\,\text{mm}$.
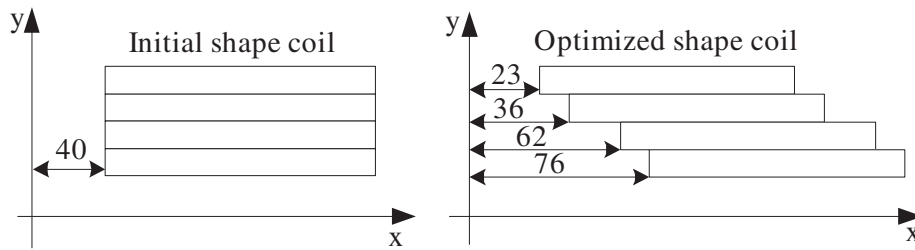
Figure 8. Comparison of cross-section shape of MgB$_2$ field coils.
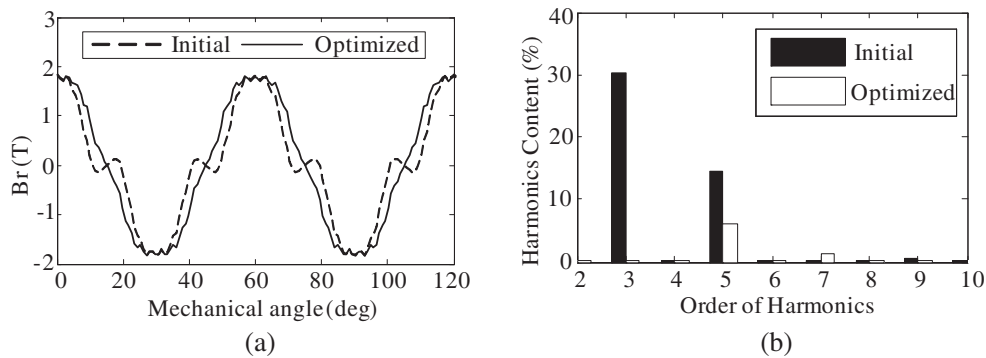
Figure 9. (a) AGMFD waveforms of non-optimized and optimized. (b) Corresponding FFT result.

The optimal cross-sectional shape of the MgB$_2$ field coils is found by a great deal of FE calculation. Fig. 8 shows the schematic illustrations of the optimized cross-section shape and the initial cross-sectional shape for MgB$_2$ field windings. Fig. 9(a) shows the AGMFD waveform of the initial structure and that of the optimized structure, and Fig. 9(b) shows the corresponding FFT results. The results show that the THD of the optimized AGMFD waveform decreases significantly from 32.48% to 7.34%.

4.3. Performance Analysis of SSG

FEM is employed to calculate the magnetic field and obtain the no-load and load performance for studying the characteristics of the initial and optimized SSG.

(1) No-Load Performance

The no-load performance of the initial and optimized SSG at 20 rpm is analyzed by using FEM. Fig. 10(a) shows the output voltage waveform of the initial structure and that of the optimized structure, and Fig. 10(b) shows the corresponding FFT results. The results show that the THD of the optimized output voltage waveform decreases from 9.72% to 4.47%.

As shown in Fig. 10, the output voltage of the optimized SSG is almost sinusoidal, and the corresponding harmonic component of output voltage is only 4.47%, which is small and can be ignored. Fig. 11 shows the cogging torque of the initial structure and that of the optimized structure. The results show that the optimized cogging torque has been significantly reduced.

The rotor has no iron, but the stator is composed of conventional copper coils and iron core. Therefore, cogging torque exists in SSG. However, the cogging torque is small. As shown in Fig. 11, the cogging torque of the optimized SSG is about 2.2 kN*m.

(2) Load Performance

Load characteristics of the initial and optimized SSG are analyzed by the transient FEM with the equivalent circuit. Load characteristics of the initial and optimized SSG are shown in Fig. 12.
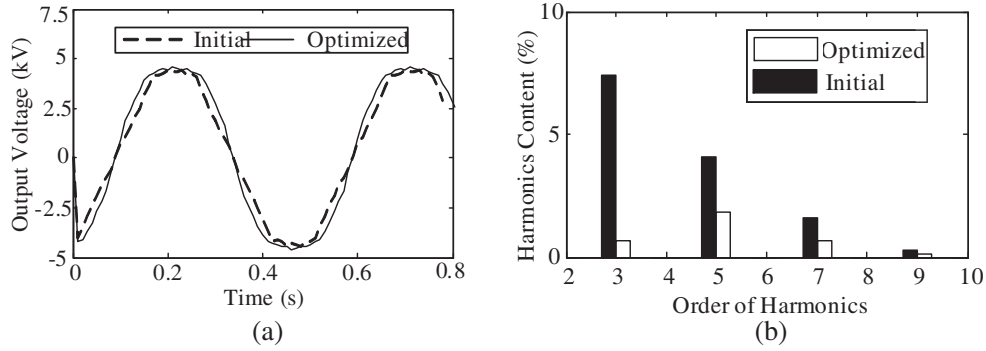
Figure 10. (a) Output voltage waveforms of initial and optimized. (b) Corresponding FFT result.
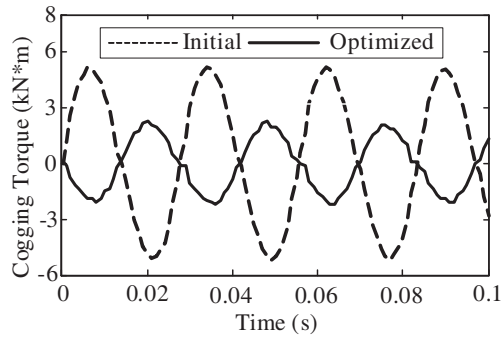
Figure 11. Cogging torques of initial and optimized.
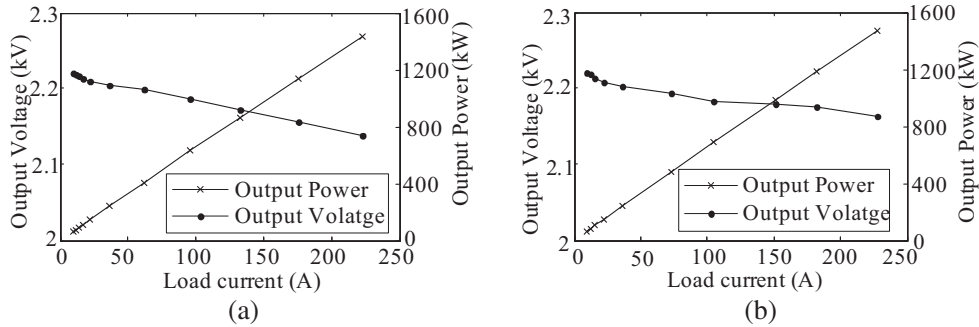
Figure 12. (a) Output power and output voltage of initial SSG. (b) Output power and output voltage of optimized SSG.

Figure 12 shows that both the initial and optimized SSGs have low voltage regulation, and their output powers are both essentially proportional to the load current. However, the voltage regulation of the optimized SSG is lower than that of the initial SSG.

The total losses generally include stator losses and rotor losses in traditional motor. However, AC losses are not a problem for the SSG, since the field winding only sees a DC field except in the fault condition and at start up/spin down [10]. Moreover, the rotor has no iron in the SSG. Therefore, the rotor losses can be ignored if the mechanical loss is neglected. The stator losses mainly include iron loss and copper loss.

The output power can be calculated by.

$$P_{out} = 3I^2 R_0 \tag{4}$$

The input power is defined as follows,

$$P_{In} = P_{out} + P_{Cu} + P_{Fe} + P_{cool} \tag{5}$$

where R_0 is the phase resistance, P_{Cu} the copper loss, P_{Fe} the core loss that can be calculated by using empirical formulas, and P_{cool} the cooling power. The cooling power typically comes in two forms: heat leaks from the surroundings and internal heat generator in the device. It mainly includes the heat loss generated by current leads, mechanical supporters and radiation in this paper.

The efficiency of SSG can be expressed by

$$\eta = (P_{out}/P_{In}) \times 100\% \tag{6}$$

The current of the armature winding is $227.3\,\text{A}$, and load resistance is $9.68\,\Omega$ when the SSG is at rated load. Under this situation, the efficiencies of the initial and optimized SSGs are calculated as 95.43% and 98.2%, respectively.

The optimized SSG has better characteristics than the initial SSG by analyzing the no-load and load performance.

5. COMPARISON

The optimized SSG is compared with a traditional synchronous generator (TSG) of the same power made by Zephyros, a wind turbine manufacturer from the Netherlands. The results are listed in Table 2.

Table 2. Comparison of SSG and TSG.

Parameters	SSG	TSG
Rated power	1.5 MW	1.5 MW
Outer diameter	1.8 m	4 m
Volume	$4.32\,\text{m}^3$	$15.1\,\text{m}^3$
Weight	9675 kg	37500 kg
Efficiency	98.2%	93.5%
Power factor	0.97	0.92

The results show that the optimized SSG has not only small size and lightweight, but also higher efficiency and higher power factor than a TSG of the same power.

From a cost perspective, the SSG needs a powerful refrigeration system, which can increase the cost. The proposed 1.5 MW SSG is not dominant on cost compared to the TSG of the same power. However, the advantage of cost will be more and more obvious for more powerful SSG. In addition, with the continued development of refrigeration technology and superconducting materials, the SSG will get cheaper and cheaper.

6. CONCLUSION

An SSG with MgB_2 field coils has been proposed for wind power. The whole refrigeration method is adopted. Not only does this method not affect the performance and efficiency of SSG, but also it makes the structure of SSG more compact and the copper loss decrease greatly. The FEM is used to optimize the SSG and obtain the no-load and load performance of the initial and optimized SSG. Finally, the optimized SSG is compared with a TSG of the same power. All of the results show that the optimized SSG has not only small size and lightweight but also higher efficiency and higher power factor than a TSG of the same power. With continued development of refrigeration technology, the SSG is well suitable for wind power system.

ACKNOWLEDGMENT

REFERENCES

1. Bladber, B., "Power electronics as efficient interface in dispersed power generation systems," *IEEE Trans. Power Electron.*, Vol. 19, No. 5, 1184–1194, Sep. 2004.

2. Qu, R., Y. Liu, and J. Wang, "Review of superconducting generator topologies for direct-drive wind turbines," *IEEE Trans. Appl. Supercond.*, Vol. 23, No. 3, 5201108, Jun. 2013.

3. IwaKuma, M., Y. Hase, T. Satou, et al., "Development of a 7.5 kW YBCO superconducting synchronous motor," *IEEE Trans. Appl. Supercond.*, Vol. 18, No. 2, 689–691, Jun. 2008.

4. Snitchler, G., B. Gamble, C. Kimg, and P. Winn, "10 MW class superconductor wind turbine generators," *IEEE Trans. Appl. Supercond.*, Vol. 21, No. 3, 1089–1092, Jun. 2011.

5. Jia, S., R. Qu, J. Li, et al., "A novel vernier reluctance fully super conducting direct drive synchronous generator with concentrated windings for wind power application," *IEEE Trans. Appl Supercond.*, Vol. 26, No. 7, 5207205, Oct. 2016.

6. Nagamatsu, J., N. Nakagawa, and T. Muranaka, "Superconductivity at 39 K in magnesium diboride," *Nature*, Vol. 410, No. 6824, 63–64, 2001.

7. Wen, H., W. Bailey, K. Goddard, and M. Al-Mosawi, "Performance test of a 100 kW HTS generator operating at 67 K–77 K," *IEEE Trans. Appl. Supercond.*, Vol. 19, No. 3, 1652–1655, Jun. 2009.

8. Leveque, J., D. Netter, B. Douine, and A. Rezzoug, "Some considerations about the cooling of the rotor of a superconducting motor," *IEEE Trans. Appl. Supercond.*, Vol. 17, No. 1, 44–51, Mar. 2007.

9. Wen, C., H. Yu, T. Hong, et al., "Coil shape optimization for superconducting wind turbine generator using response surface methodology and particle swarm optimization," *IEEE Trans. Appl. Supercond.*, Vol. 24, No. 3, 5202404, Jun. 2014.

10. Jiang, Q., M. Majoros, Z. Hong, A. M. Campbell, and T. A. Coombs, "Design and AC loss analysis of a superconducting synchronous motor," *Supercond. Sci. Technol.*, Vol. 19, 1164–1168, 2006.